Songklanakarin J. Sci. Technol.
36 (1), 107-113, Jan. - Feb. 2014

SJST SONGKLANAKARIN JOURNAL OF SCIENCE AND TECHNOLOGY
http://www.sjst.psu.ac.th

Original Article

Performance analysis of a water pumping system supplied by a photovoltaic generator with different maximum power point tracking techniques

Bhavnesh Kumar*, Yogesh K Chauhan, and Vivek Shrivastava

School of Engineering, Gautam Buddha University,
Greater Noida, 201308 India.

Received 13 September 2012; Accepted 10 October 2013

Abstract

In this paper investigations are made with different maximum power point tracking (MPPT) techniques for a photovoltaic generator (PVG). The PVG is used to supply an induction motor driving a centrifugal pump. Boost converter and inverter are connected in between PVG and motor for power conditioning. Three MPPT techniques are designed and compared. These techniques are incremental conductance (IC), constant voltage controlled (CVC) and fuzzy based perturbation and observation (FPO). Rule Base of FPO is designed with nine rules only, so that it can be implemented on limited memory and speed processors. System performance is analyzed with the help of developed simulation models. A comparative study of these techniques is also summarized. The obtained simulation results indicate that FPO scheme yields better performance.

Keywords: Constant voltage controller (CVC), Fuzzy logic, Incremental conductance (IC), induction motor, Perturbation and Observation (PO), PV generator

1. Introduction

Despite of high generating cost, photovoltaic (PV) energy generation has given quite a lot of attention and encouragement. This is due to its capability to accommodate the three major challenges the world is facing: (1) energy deficit, (2) depleting conventional energy sources, and (3) environmental concerns (Kuo and Liang, 2001). The use of PV power can also be economical, particularly in areas where grid connected electricity is not readily available. Furthermore, as the need of water and sun's availability are interdependent so it becomes more suitable to use PV power for water pumping applications in remote areas (Kun *et al.*, 2012; Mekhilef *et al.*, 2013).

PV array captures the solar energy and converts into the useful form. However, low conversion efficiency and extraction of maximum available power from PV array are two major concerns. The first concern is addressed by research that is generally directed towards the engineering materials. For second concern, the use of maximum power point tracking (MPPT) technique is unavoidable due to the non-linear characteristics of PV arrays (Gao *et al.*, 2013; Kuo *et al.*, 2001).

In the literature different MPPT techniques have been discussed which can be broadly categorized into a) incremental conductance (IC) technique (Fangrui Liu *et al.*, 2008; Safari and Mekhilef, 2011) and b) perturb and observe (PO) technique (Femia *et al.*, 2005; Sera *et al.*, 2013). It is reported that the IC technique offers a good tracking capability, however the implementation is more complex. The implementation of PO technique is much simpler, but the technique fails during rapid changes of the weather conditions. For its improvement, conventional PO techniques are used in conjunction with AI algorithms. Fuzzy logic (FL), due to its well known advantageous features, is preferred among various AI techniques for control applications (Benlarbi *et al.*, 2004; Algazar *et al.*, 2012).

* Corresponding author.
Email address: kumar_bhavnesh@yahoo.co.in

In general, there is a direct relation among the size of the rule base and the performance of the FL based system. The increase in the size of a rule base can increase the complexity. In most of the works on MPPT authors had used the reduced rule base of twenty five (25) rules in comparison to the forty nine (49) rules (Kottas *et al.*, 2006; Larbes *et al.*, 2009; Alajmi *et al.*, 2011; Messai *et al.*, 2011).

Elgendy *et al.* (2010) presented a constant voltage controller (CVC) based on MPPT technique. The technique requires the measurement of the array voltage only and was easily implementable with both analogue and digital circuits. The scheme offers better energy utilization only at low cell temperatures. However, more sophisticated MPPT algorithms are required to improve the performance at normal temperature and fast varying irradiance level.

The aim of this paper is to present a detailed analysis of a water pumping system powered from a PV source. Extensive simulation study has been carried out by developing MATLAB/Simulink model of the complete system. The system is assisted with MPPT technique for maximum power extraction. In this paper, performance of PV based water pumping system with proposed fuzzy based perturb and observe (FPO) MPPT technique is presented and compared with the IC and CVC techniques at varying weather conditions.

2. System Description and Modeling

The system under investigation consists of a PV array, power conditioning unit, induction motor, and centrifugal pump. A simple, but accurate model of a PV array and centrifugal pump are developed in order to simulate the complete system. All components are modeled separately and then joined together. A schematic diagram of the system under investigation is shown in Figure 1.

2.1 PV array

In order to meet the load requirements, the number of PV modules are interconnected and called as PV array. PV modules are formed by interconnecting the solar cell in series/parallel combinations.

For describing the electrical behavior of solar cell different mathematical models have been reported in the literature. Perhaps, the simplest equivalent model is one diode model as shown in Figure 2. The output voltage of PV generator formed by such equivalent model can be given as:

$$V_{pvg} = \left(\frac{nkT_C}{q}\ln\left(\frac{I_{sc}+I_r-I_{pvg}}{I_r}\right)-I_{pvg}R_s\right) \quad (1)$$

where V_{pvg} and I_{pvg} are output voltage and currents of the PV generator, respectively, R_s is the cell resistance, I_{sc} is the photocurrent or short circuit current, I_r is the reverse saturation current of diode, q is the electron charge, k is Boltzmann constant, T_r is the reference operating temperature of cell and n is the ideality factor. The effect of variation in operating temperature due to the variation in irradiance level is also incorporated.

2.2 Power conditioning unit

In this work, a two stage power conditioning unit is used. In the first stage a boost converter as shown in Figure 3 is used to implement the MPPT scheme for the PV generator. During steady state operations, the input-output relationship of boost converter is given by:

$$\frac{V_0}{V_{in}} = \frac{1}{1-D} \quad (2)$$

In the second stage, a three phase inverter is employed to convert the available DC into AC for feeding the induction motor. The output is controlled by a PWM control circuit forcing the voltage frequency ratio to remain constant.

2.3 Induction motor

Several types of DC and AC motors are available for photovoltaic based water pumping applications. Various factors such as size, reliability, availability, and price are

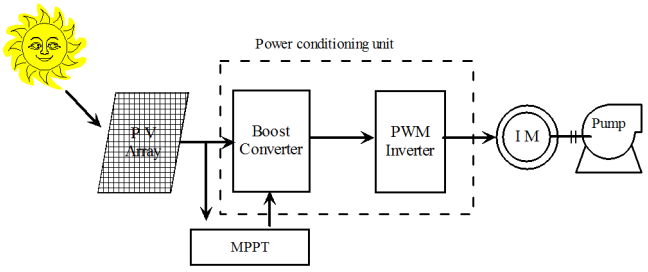

Figure 1. Schematic diagram of the constant voltage controlled system.

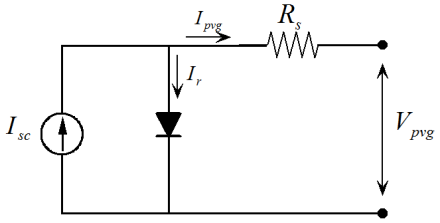

Figure 2. Equivalent circuit of solar cells.

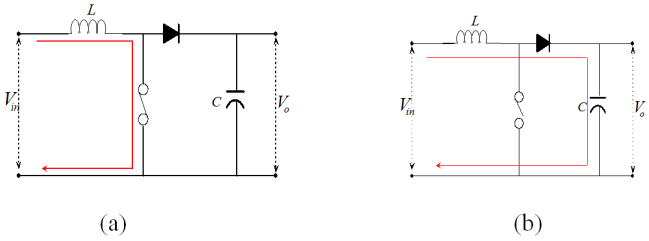

Figure 3. Boost converter with (a) switch is closed and (b) switch if open.

considered during the selection of motor. Induction motors due to inherent advantages are preferred over dc motors for water pumping application (Bhat *et al.*, 1987). The dynamic equivalent circuit of a three phase induction motor expressed in *d-q* synchronously rotating reference frame is shown in Figure 4.

The electromagnetic torque developed by an induction motor is given by:

$$T_e = \frac{3}{2}\frac{P}{2}L_m(I_{qs}I_{dr} - I_{ds}I_{qr}) \quad (3)$$

The mechanical part modeling of an electric motor is given by:

$$T_e = Jp\omega_m + B\omega_m + T_L \quad (4)$$

where J is the total inertia of motor shaft, B is the friction coefficient, and T_L is the load torque.

2.4 Centrifugal pump

The selection of the size of the pump is crucial as it represents the mechanical load of the induction motor and it identifies the ratings of the other system components. For this work a centrifugal pump of nominal power (P_n) = 1.5 kW and nominal speed (ω_n) = 145.5 rad/sec is used.

A centrifugal pump load is generally modeled in the form of a load torque requirement of a motor shaft. This load torque depends on the process requirements of head to be overcome, flow rate requirement, and the operating speed. The torque speed characteristic of the motor for a pump load can be given by:

$$T_L = T_P = K\omega_r^{\,2} \quad (5)$$

Here K is defined in terms of nominal pump power P_n and speed ω_n as:

$$K = \frac{P_n}{\omega_n^{\,3}} \quad (6)$$

3. MPPT Techniques

All three MPPT techniques, namely PO, IC and CVC, are basically based on the same concept of regulating the PV array's voltage to follow an optimal set point, which represents the voltage of maximum power operating point.

3.1 Incremental conductance

For this work, IC based MPPT technique is designed on the conventional approach of tracking the zero slope region ($dP/dV = 0$) on the power curve.

$$\text{Since } \frac{dP}{dV} = \frac{d(IV)}{dV} = I + V\frac{dI}{V} \cong I + V\frac{\Delta I}{\Delta V} \quad (7)$$

For MPP tracking instantaneous conductance (*I/V*) and the incremental conductance (Δ*I*/Δ*V*) are compared until the relationship (Δ*I*/Δ*V*) = -(*I*/*V*) is satisfied. A fixed gain PI controller is employed to adjust the duty ratio of a boost converter.

3.2 Constant voltage controlled

This technique utilizes the fact that region of MPP for all the operating conditions for a PV generator vary in a narrow band of voltage range. So, a fixed value for the MPP voltage equal to 180 V is selected as the reference voltage in this work. This value is used as a set point for the feedback control loop. Here also, a fixed gain PI controller is employed to adjust the duty ratio of a boost converter.

3.3 Fuzzy based perturbation and observation

In this work, a FL controller is used instead of a conventional PI controller to adjust the duty ratio. A MPP locator is based on the PO technique of perturbing the array operating voltage. A FL controller is proposed to overcome the demerits such as initial tuning and detuning (with change in operating conditions) of conventional PI controller. A FL controller importantly consists of three stages: fuzzification, rule base table lookup, and defuzzification. The inputs of the FL controller are:

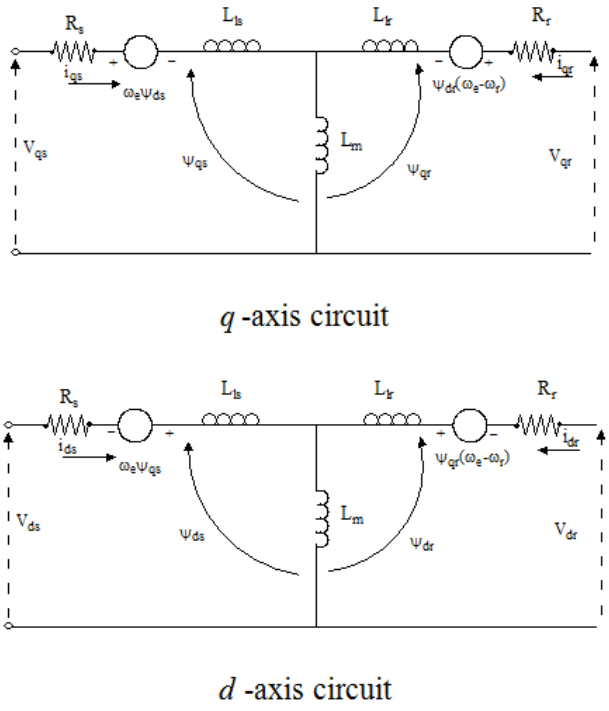

Figure 4. Dynamic equivalent circuits of a machine. R_s & R_r are the stator and rotor resistances resp., L_{ls} & L_{lr} are the stator and rotor leakage inductances respectively, L_m is the mutual inductance, V_{ds} & V_{dr} are the *d*-axis stator and rotor voltages respectively, V_{qs} & V_{qr} are *q*-axis stator and rotor voltages resp., ψ_{qs} & ψ_{qr} are the *q*-axis stator and rotor flux linkages resp., ψ_{ds} & ψ_{dr} are the *d*-axis stator and rotor flux linkages respectively.

$$E(k) = \frac{P_{pvg}(k) - P_{pvg}(k-1)}{V_{pvg}(k) - V_{pvg}(k-1)} \quad (8)$$

$$\Delta E = E(k) - E(k-1) \quad (9)$$

and the output control signal is given as:

$$\Delta D = D(k) - D(k-1) \quad (10)$$

where $E(k)$ is the error, $\Delta E(k)$ is the change in error, and ΔD is change in duty cycle of boost converter.

The inputs/output of the FL controller is normalized using scaling factors chosen by *trial and error* method. Scaling factors play an important role in fixing the optimization problem. Trapezoidal and triangular shape membership functions for both inputs and output shown in Figure 5 were selected. The universe of discourse is divided into three fuzzy subsets functions: NE (negative), ZE (zero) and PE (positive). A total of nine rules are formulated and summarized in Table 1. The output before being given to the boost converter is defuzzified using a center of area method.

Table 1. Rule base for FPO.

$\Delta E(k)$	$E(k)$		
	NE	ZE	PE
NE	ZE	NE	NE
ZE	NE	ZE	PE
PE	PE	PE	ZE

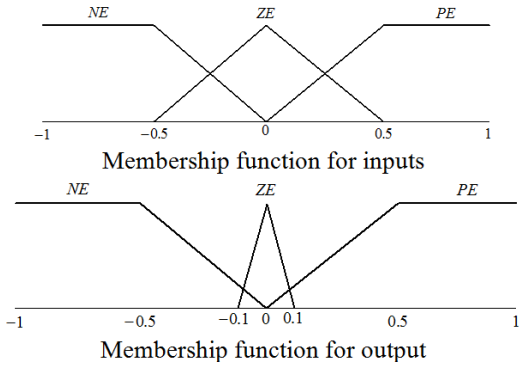

Figure 5. Membership functions used for inputs/output.

4. Results and Discussion

To study the steady state and transient performance of the system under investigation the system is designed using Equations 1 to 9 in the Simulink/MATLAB environment. The results were obtained after simulating the system in a discrete mode with a sampling frequency of 20 kHz under various operating conditions that are discussed in the following sections.

4.1 PV array characteristics

The P-V and I-V characteristics of the photovoltaic array are shown in Figure 6(a) and 6(b), respectively, for insolation levels of 1,000 W/m^2, 800 W/m^2, 600 W/m^2, and 400 W/m^2 at a constant temperature of 20°C. The increase in insolation level from 400 W/m^2 onwards results in an increase of both open circuit voltage and short circuit current. The corresponding open circuit voltage, short circuit current and maximum power available is shown in Table 2 for given insolation levels.

The P-V and I-V characteristics of photovoltaic array are shown in Figure 7(a) and 7(b), respectively, for different operating temperatures of 0°C, 10°C, 20°C, 30°C, 40°C at a constant insolation level of 1,000 W/m^2. The increase in temperature results into an increase of the open circuit voltage, and no variation of short circuit current. The variation of open circuit voltage, short circuit current and maximum power available at given temperatures is shown in Table 3.

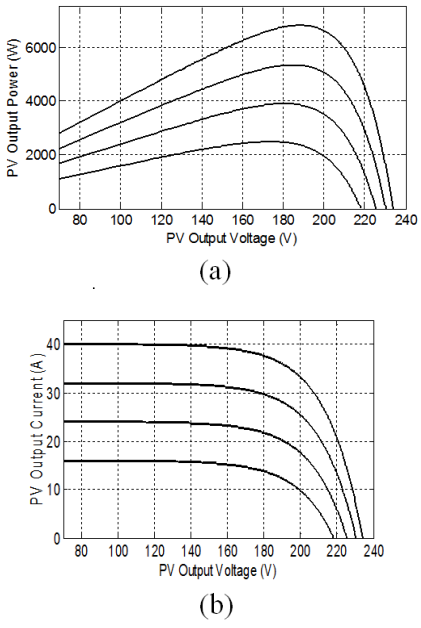

Figure 6. (a) P-V (b) I-V characteristic for different insolation levels.

4.2 Performance analysis with IC technique

The performance of system employing a conventional IC technique of MPP tracking is investigated. The responses of photovoltaic array parameters (V_{pvg}, I_{pvg}, P_{pvg}), boost converter parameter (V_{bst}) and motor driven pump load parameters (I_{sm}, T_{em}, ω_{rm}) shown in Figure 8 are analyzed. Once the steady state of system is achieved without motor driven pump load, the said load is connected at 1.0 sec., which is resulted into change of system dynamics. With the connection of load, the PV array side parameters remain almost

Table 2. Open circuit voltage, short circuit current and maximum power for different insolation levels.

Insolation level	Max. Current	Max. Voltage	Max. Power
1,000	40.15	233.9	6,823
800	32.17	230.2	5,351
600	24.19	225.3	3,905
400	16.21	218.1	2,498

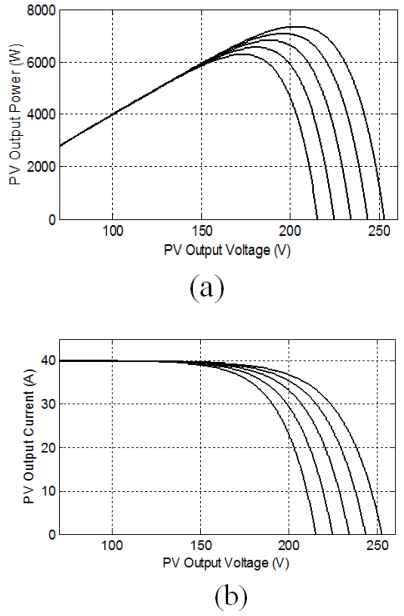

Figure 7. Characteristic for different temperature level (a) P-V and (b) I-V.

constant. The V_{bst} decreases slightly from 363.7 V and settled to 334.1 V. After a brief starting transient period, the i_{sm} and T_{em} attain steady state values. After connection of motor driven pump, the ω_{rm} gradually increases to steady state value of 130.4 rad/s.

4.3 Performance analysis with CVC

Figure 9 shows the performance responses of the PV based system employing a CVC for MPP Tracking. The responses of Vpvg, I_{pvg}, P_{pvg}, V_{bst}, I_{sm}, T_{em}, ω_{rm} are obtained in time domain and then analyzed. At the start, the induction motor is under no–load conditions and after attaining steady state the pump load is connected at a time t=1.0 sec to the motor. When the load is connected, the PV array parameters remain almost constant and V_{bst} decreases slightly from 367.7 V and settled at 331.5 V. After a brief starting transient period, the i_{sm} and T_{em} attain steady state values of 8.3 A and 5.1 N-m respectively. After connection of the motor driven pump ω_{rm} gradually increases to steady state value of 129.5 rad/s.

4.4 Performance analysis with FPO

Figure 10 shows the responses of the system employing a FLC for MPP tracking. The responses of Vpvg, I_{pvg}, P_{pvg}, V_{bst}, I_{sm}, T_{em}, ω_{rm} are obtained under constant temperature and insolation level. The system under observation is brought from no–load condition to loaded condition at time t=1 sec by connecting a pump load. Under loaded condition, the PV array side parameters are almost constant and V_{bst} decreases slightly from 363.6 V and settled to 330.9 V. After a brief starting transient period, the i_{sm} and T_{em} attain steady state values of 7.8 A and 5.2 N-m respectively. After connection of the motor driven pump ω_{rm} gradually increases to steady state value of 132.5 rad/sec.

The responses obtained for analyzing the performance of the system under consideration with three of MPPT techniques individually are summarized in Table 4 for the comparative study. It is evident that the FPO based MPPT scheme has a better performance

5. Conclusion

Detailed simulation analysis of a 3-phase induction motor driven water pumping system sourced by a PV generator is presented. A minimal rule base FL controller for MPP tracking is also designed. The performance of the system is

Table 3. Open circuit voltage, short circuit current and maximum power at different temperature level

Temperature Level	Max. Current	Max. Voltage	Max. Power
0	40.12	252.6	7,359
10	40.13	243.2	7,092
20	40.15	233.9	6,823
30	40.16	224.5	6,555
40	40.17	215.2	6,286

Table 4. System performance with different MPPT techniques

MPPT scheme	Instantaneous values (t=0.8 sec) when motor is at rest							Instantaneous values (t=2.4 sec) when motor is running with load						
	Vpvg	Ipvg	Ppvg	Vbst	I_{sm}	T_{em}	ω_{rm}	Vpvg	Ipvg	Ppvg	Vbst	I_{sm}	T_{em}	ω_{rm}
IC	186.1	36.6	6819	363.6	0	0	0	185.4	36.7	6816	330.9	-7.8	5.6	132.5
CVC	181.2	37.4	6777	367.7	0	0	0	180.1	37.5	6763	331.5	-8.3	5.1	129.5
FPO	187.8	36.4	6823	363.7	0	0	0	187.8	36.5	6823	334.1	-8.2	5.2	130.4

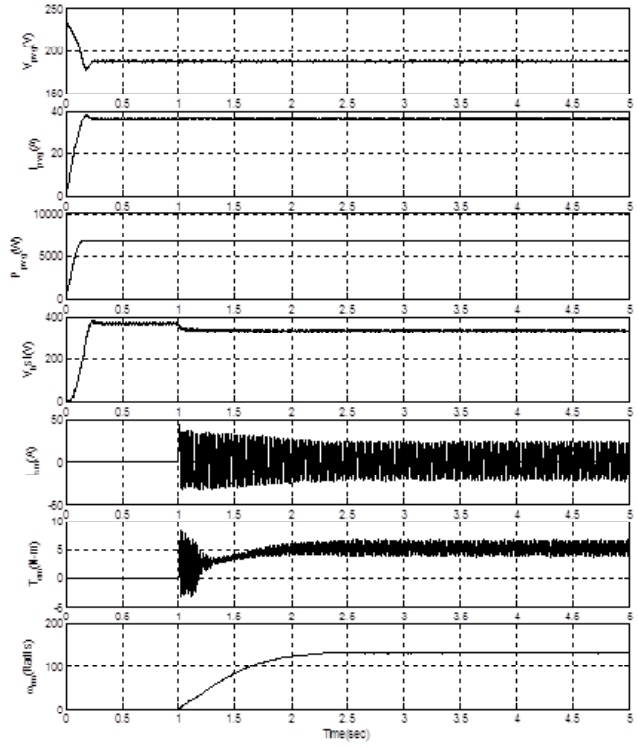

Figure 8. Responses using IC technique for PV based water pumping system

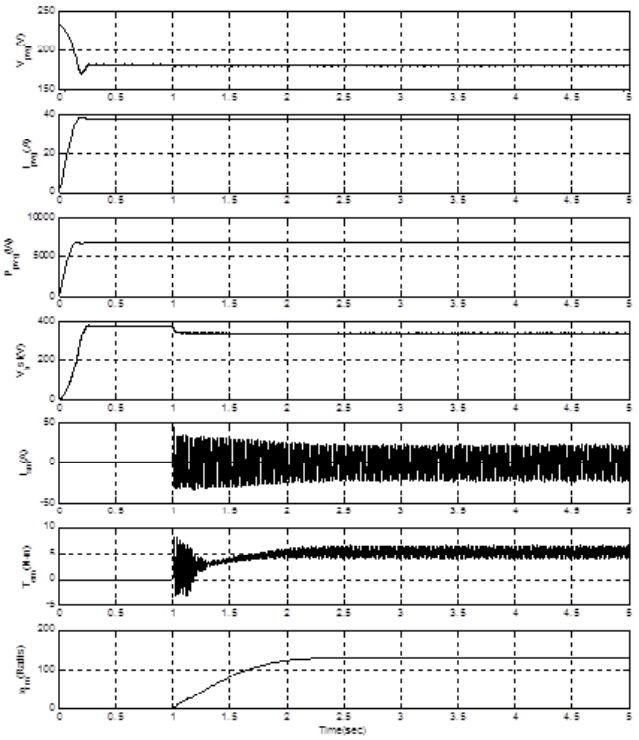

Figure 9. Responses using CVC technique for PV based water pumping system.

obtained with three different MPPT techniques, namely incremental conductance, fuzzy based perturbation and observation, and constant voltage control. The performance of the FPO is found superior in comparison to the other two techniques.

References

Alajmi, B.N., Ahmed, K.H., Finney, S.J. and Williams, B.W. 2011. Fuzzy logic control approach of a modified hill-climbing method for maximum power point in microgrid standalone photovoltaic system. Institute of Electrical and Electronics Engineers Transactions on Power Electronics. 26(4), 1022-1030.

Altas, I.H. and Sharaf, A.M. 2008. A novel maximum power fuzzy logic controller for photovoltaic solar energy systems. Renewable Energy. 33(3), 388-399.

Algazar, M.M., AL-monier, H., Abd EL-halim, H. and Salem, M. 2012. Maximum power point tracking using fuzzy logic control. International Journal of Electrical Power and Energy Systems. 39(1), 21-28.

Benlarbi, K., Mokrani, L. and Nait-Said, M. 2004. A fuzzy global efficiency optimization of a photovoltaic water pumping system. Solar Energy. 77(2), 203-16.

Bhat, S.R., Pittet, A. and Sonde, B.S. 1987. Performance Optimization of Induction Motor-Pump System Using Photovoltaic Energy Source. Institute of Electrical and Electronics Engineers Transactions on Industrial Applications. 23(6), 995-1000.

Elgendy, M.A., Zahawi, B. and Atkinson, D.J. 2010. Comparison of Directly Connected and Constant Voltage Controlled Photovoltaic Pumping Systems. Institute of Electrical and Electronics Engineers Transactions on Sustainability Energy. 1(3), 184-192.

Femia, N., Petrone, G., Spagnuolo, G. and Vitelli, M. 2005. Optimization of perturb and observe maximum power point tracking method. Institute of Electrical and Electronics Engineers Transactions on Power Electronics. 20(4), 963-973.

Gao, X., Li, S. and Gong, R. 2013. Maximum power point tracking control strategies with variable weather parameters for photovoltaic generation systems. Solar Energy. 93, 357-367.

Kun, D., XinGao, B., HaiHao L. and Tao, P. 2012. A MATLAB-Simulink-Based PV Module Model and Its Application Under Conditions of Nonuniform Irradiance. Institute of Electrical and Electronics Engineers Transactions on Energy Conversion. 27(4), 864 – 872.

Kuo, Y.C. and Liang, T.J. 2001. Novel maximum-power-point-tracking controller for photovoltaic energy conversion system. Institute of Electrical and Electronics Engineers Transactions on Industrial Electronics. 48(3), 594–601.

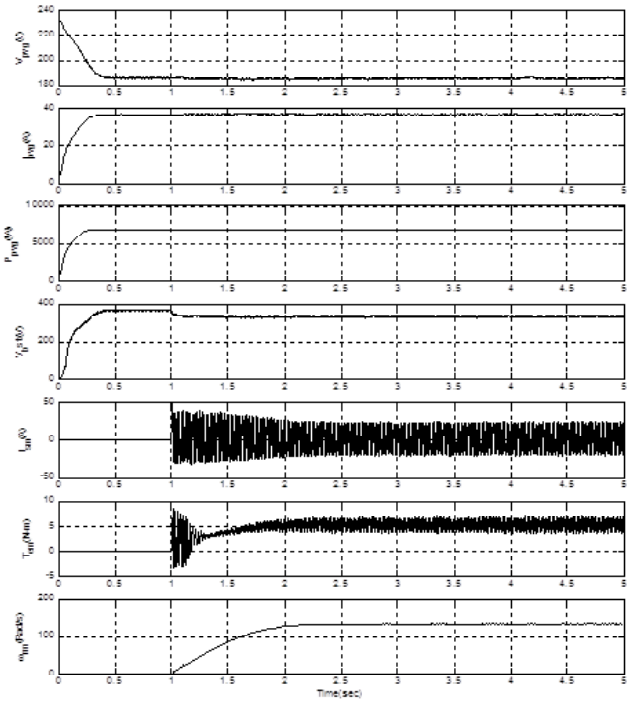

Figure 10. Responses using FPO for PV based water pumping system.

Kottas, T.L., Boutalis, Y.S. and Karlis, A.D. 2006. New maximum power point tracker for PV arrays using fuzzy controller in close cooperation with fuzzy cognitive networks. Institute of Electrical and Electronics Engineers Transactions on Energy Conversion. 21(3), 793–803.

Liu, F., Duan, S., Liu, F., Liu, B. and Kang, Y. 2008. A Variable Step Size INC MPPT Method for PV Systems. Institute of Electrical and Electronics Engineers Transactions on Industrial Electronics. 55(7), 2622-2628.

Larbes, C., Ait Cheikh, S.M., Obeidi, T. and Zerguerras, A. 2009. Genetic algorithms optimized fuzzy logic control for the maximum power point tracking in photovoltaic system. Renewable Energy. 34(10), 2093-2100.

Mekhilef, S., Faramarzi,S. Z., Saidur, R. and Salam, Z. 2013. The application of solar technologies for sustainable development of agricultural sector. Renewable and Sustainable Energy Reviews. 18, 583-594.

Messai, A., Mellit, A., Massi, P.A., Guessoum, A. and Mekki, H. 2011. FPGA-based implementation of a fuzzy controller (MPPT) for photovoltaic module. Energy Conversion Management. 52(7), 2695-2704.

Safari, A. and Mekhilef, S. 2011. Simulation and Hardware Implementation of Incremental Conductance MPPT With Direct Control Method Using Cuk Converter. Institute of Electrical and Electronics Engineers Transactions onIndustrial Electronics. 58(4), 1154-1161.

Sera, D., Mathe, L., Kerekes, T., Spataru, S.V. and Teodorescu, R. 2013. On the Perturb-and-Observe and Incremental Conductance MPPT Methods for PV Systems. Institute of Electrical and Electronics Engineers Journal of Photovoltaics. 3(3), 1070 – 1078.

Appendix A

Parameters of 3-phase Induction Motor:

3 HP, 4 pole, 220 V, 50 Hz, Stator Resistance (R_s) = 0.435 Ω, Rotor Resistance (R_r) = 0.816 Ω, Stator Inductance (L_{ls}) = 2.0 mH, Rotor Inductance (L_{lr}) = 2.0 mH, Mutual inductance (L_m) = 69.3 mH, Inertia Constant (J) = 0.02 Kg-m^2, Friction Factor (F) = 0.002 N-m-s